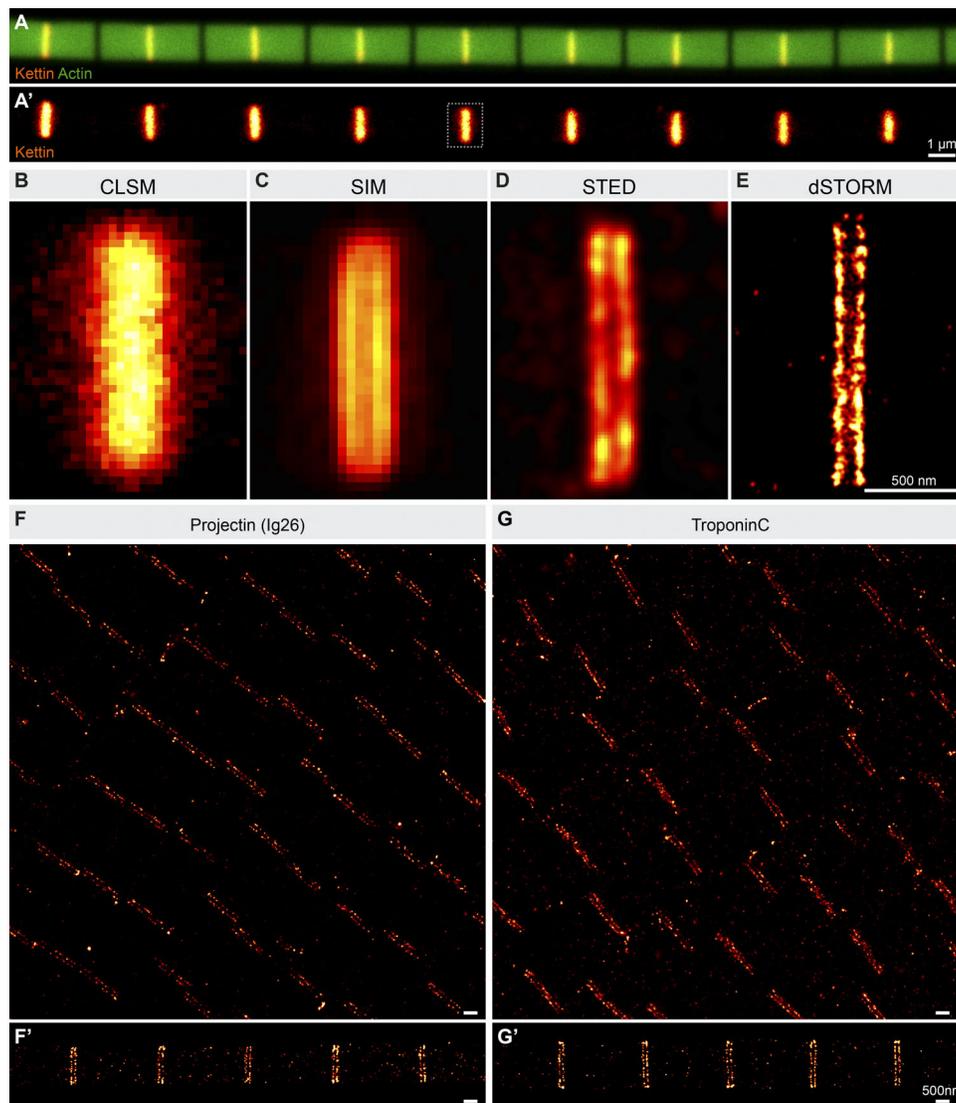# Supplemental material

Figure S1. **Individual myofibrils of the *Drosophila* IFMs are ideal for dSTORM imaging. (A and A')** Confocal imaging of the individual myofibrils nicely reveals actin organization and Kettin accumulation at the Z-disk. Scale bar, 1 µm. **(B–E)** The Kettin signal at the Z-disk appears as a single band with CLSM (B) that can be resolved into two individual bands with superresolution approaches such as SIM (C), STED (D), and dSTORM (E), of which dSTORM clearly provides the highest resolution. Scale bar, 500 nm. **(F–G')** Comparison of the nanoscopic localization of Projectin (Ig26) and TnC in dissected intact flight muscles (F and G) with that in individual myofibrils (F' and G') reveals a highly similar pattern. Scale bars, 500 nm.
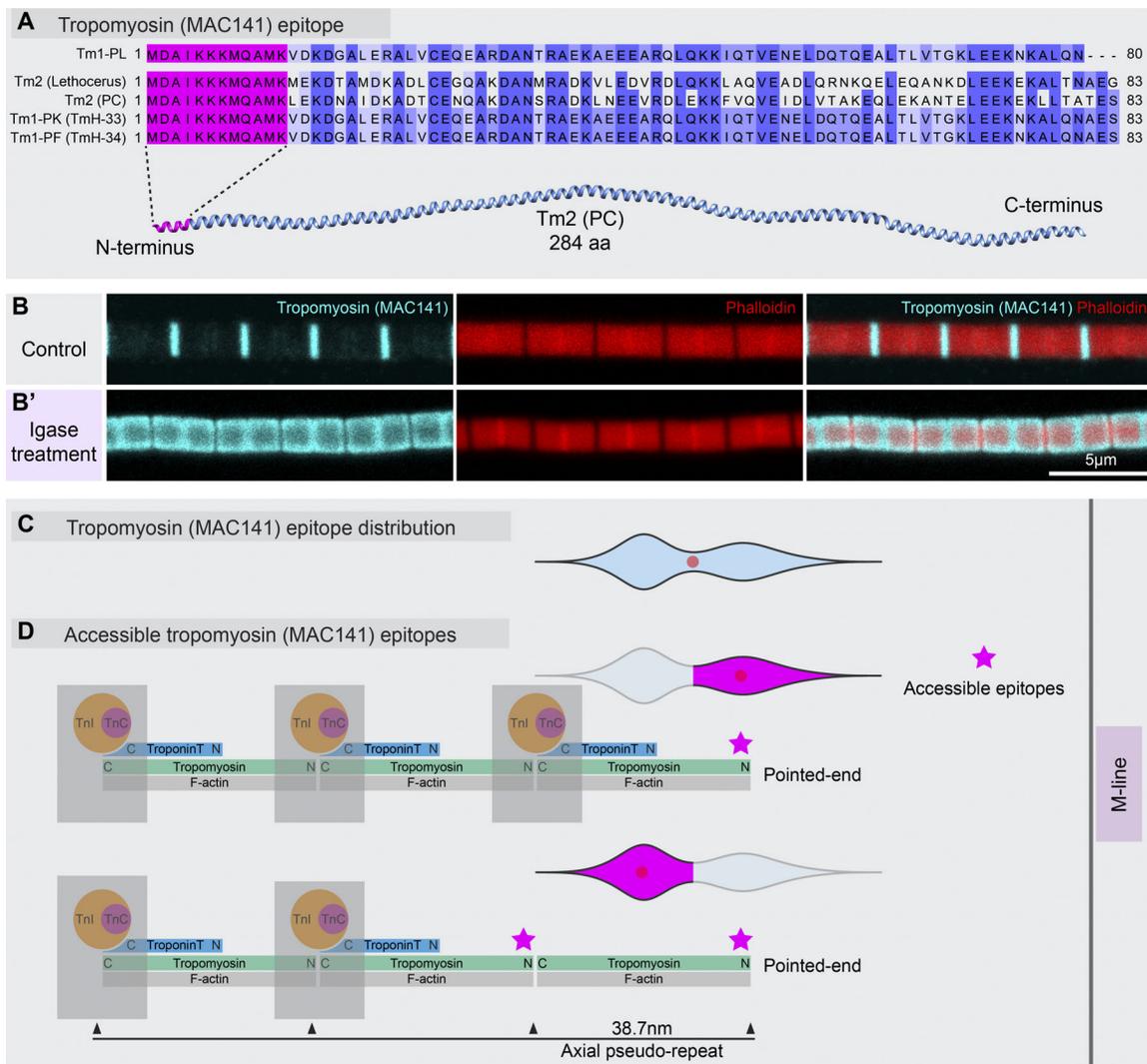
Figure S2. **Tm (MAC141) epitope position and distribution. (A)** The epitope recognized by the monoclonal MAC141 antibody has been restricted to an 80-aa-long N-terminal sequence in Tm1-PL, and this antibody is known to recognize all IFM-specific Tm isoforms (Tm2, TmH-33, and TmH-34). Sequence comparison suggests that the MAC141 epitope is most likely within a 12-aa-long conserved N-terminal region (highlighted in magenta). **(B)** MAC141 staining of wild-type IFM myofibrils displays a strong signal in the H-zone and a faint signal in the A-band. Nanoscopy revealed that the H-zone accumulation corresponds to a double line structure close to the pointed ends. This suggests that the epitope recognized by MAC141 is close to the pointed ends but largely masked along the rest of the thin filaments. **(B')** Myofibrils treated with the Igase enzyme to remove the hydrophobic extensions of TmH-34, thereby loosening up the Tn bridges, exhibit a nearly uniform MAC141 staining along the A-bands. This observation supports the idea that the epitope is masked in the A-band and it is located on the N-terminus. Scale bar, 5 μm. **(C and D)** Unlike in the I-band where Tm exhibit a double-line-type distribution with one single peak on both sides of the Z-line, the MAC141 signal in the H-zone appears as a double peak on either side of the M-line (schematized in C). The M-ward peak of the doublet corresponds exactly to the pointed-end region, whereas the other marks the middle of the most proximal axial repeat (D). The I-band distribution and position of the M-ward H-zone peak is entirely consistent with an N-terminal epitope localization. With regard to the peak in the middle of the most proximal axial repeat, we propose that it could be the average position of the two most M-ward epitopes by assuming that the most proximal Tn complex is missing from some of the thin filaments, which makes those epitopes accessible (stars).
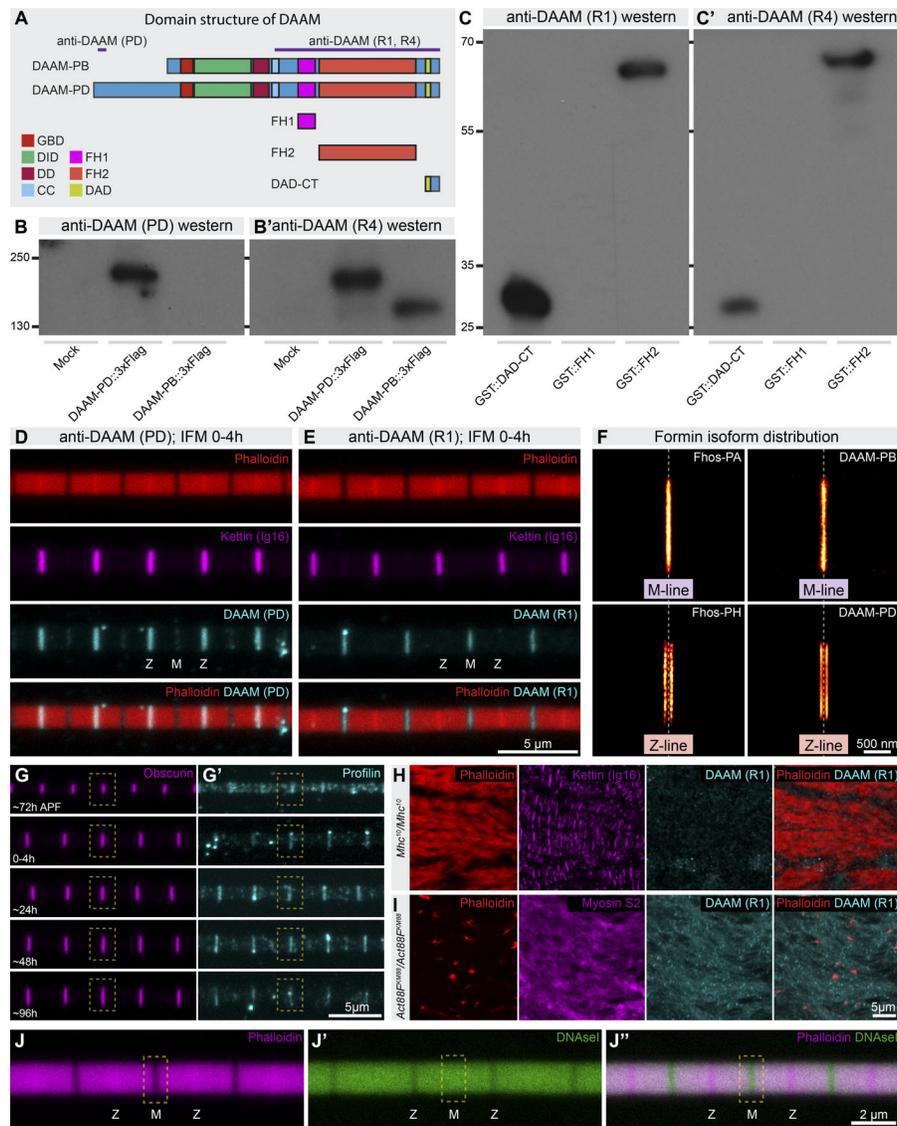
Figure S3. **The short and long isoforms of DAAM and the localization of Profilin. (A)** Domain structure of the two DAAM isoforms, PB and PD, expressed in the IFM. Note that the two isoforms are completely overlapping, while the PD isoform contains an N-terminal extension of 310 aa. The anti-DAAM (PD) serum was raised against an N-terminal, PD isoform–specific peptide, whereas the (R1) antibody was raised against a C-terminal region of the protein, present in both isoforms. **(B and B')** Western blots show that, as expected, the (R4) antibody (raised against the same sequences as R1) recognizes the short (PB) and long (PD) isoform, while the anti-DAAM (PD) recognizes only the long isoform from S2 cell lysates transfected with DAAM-PB– or DAAM-PD–expressing constructs. **(C and C')** Western blots with bacterially expressed proteins reveal that R1 and R4 both recognize the FH2 and DAD-CT regions but not the FH1 domain. It is of note that R1 appears to exhibit a much higher affinity for DAD-CT than R4. **(D and E)** Anti-DAAM (PD) staining in a 0–4 h IFM reveals a strong accumulation at the Z-disk and a weak signal at the M-line; conversely, (R1) displays a strong signal at the M-line and a very weak if any enrichment at the Z-disk. Thus, it appears that although (R1) recognizes both isoforms in denaturing conditions (i.e., after SDS-PAGE), when used for immunohistochemistry, it is specific for the short isoform. In addition, these results indicate that in these young IFMs, the PD isoform is enriched at the Z-disk, whereas the PB isoform accumulates at the M-line. Scale bar, 5 µm. **(F)** Comparison of the nanoscopic distribution of the two Fhos and two DAAM isoforms in the IFM demonstrates that the short isoforms (Fhos-PA and DAAM-PB) are enriched in a narrow stripe at the M-line, while the long isoforms (Fhos-PH and DAAM-PD) accumulate in two stripes along the Z-line. This differential distribution is likely to indicate an isoform specific in vivo function at the Z-disk versus the M-line, for example the short isoforms promote pointed end elongation while the long isoforms are involved in barbed end dynamics. Scale bar, 500 nm. **(G and G')** Developmental analysis of Profilin accumulation in the IFM. Whereas former work suggested that Profilin accumulates at the Z-disk, we found that, in addition to a weak staining along the entire myofibril, the bulk of the protein is enriched at the M-line (indicated by the colocalization with Obscurin) in the IFM of 24-h-old adults. To rule out the possibility that Profilin expression displays a different pattern during development, we examined its distribution in two earlier (72 h after puparium formation [APF] and 0–4 h adult) and two later (48 h and 96 h adult) developmental time points. This analysis confirmed the M-line association at each developmental stage, although the enrichment looked somewhat less specific in 72-h-APF myofibrils. Scale bar, 5 µm. **(H and I)** Sarcomere association of DAAM depends on Mhc. **(H)** Confocal images show that DAAM localization in an *Mhc*-null mutant myofibril is virtually lost. **(I)** In *Act88F*-null mutant IFMs, a residual DAAM accumulation is clearly visible. In agreement with its nanoscopic protein distribution at the M-line, these data suggest that myofibril association of at least the short isoform of DAAM, recognized by R1 in 0–4 h IFM, primarily depends on Mhc and not on actin. **(J–J'')** Myofibrillar G-actin distribution was visualized with deoxyribonuclease I (DNaseI) staining, which revealed a nearly uniform localization along the entire myofibril but at the Z-disk, where the staining is much weaker than elsewhere. This result clearly confirms the presence of G-actin in the H-zone. Scale bar, 5 µm.

Table S1. **List of primary antibodies used in this study**

Protein target	Name	Antigen	Host species	Dilution	Source/supplier	Reference
Actin	Actin (rat)	Monoclonal antibody reacts with actin and arthrin	Rat	1:200	Babraham MAC 237	Lakey et al., 1990
Actin	Actin (C4)	Epitope appears to be located in the N-terminus, possibly near amino acids 50–70	Mouse	1:200	Cedarlane Laboratories	
Cpa	Cpa	Antibody was raised against full-length Cpa sequence	Rabbit	1:100	Florence Janody	Amândio et al., 2014
DAAM	DAAM (R1)	Antibody was raised to the C-terminal half (C-DAAM) of the protein; "R1"	Rabbit	1:1,000	Our laboratory	Matusek et al., 2006
DAAM	DAAM (PD)	Antibody was raised against an N-terminal polypeptide corresponding to amino acid residues 26–43 of the DAAM-PD; "PD756 INEP"	Rabbit	1:1,000	Our laboratory	This study
Fhos	Fhos	Antibody was raised to the 93 C-terminal residues of the Fhos protein	Rat	1:100	Ben-Zion Shilo	Shwartz et al., 2016
FLN	FLN (C-term)	Epitope is located in the last 90 C-terminal residues; "43-D"	Rabbit	1:100	Thomas Hays	Li et al., 1999
FLN	FLN (N-term)	Epitope is located in the N-terminus (residues 189–482)	Rat	1:100	Mirka Uhlirova	Külshammer and Uhlirova, 2013
FliI	FliI	Antibody was raised to the N-terminus of FliI (human origin; "(116.40): sc-21716"	Mouse	1:50	Santa Cruz Biotechnology	
Kettin	Kettin (Ig34)	Epitope is located in the Ig34–Ig35 region; "K40"	Rabbit	1:200	Belinda Bullard	Kulke et al., 2001
Kettin, Sls700	Kettin (Ig16)	Epitope is located in the linker-Ig16-linker region	Rat	1:200	Babraham MAC 155	Lakey et al., 1990
Mhc	Myosin S2	Monoclonal antibody reacts with subfragment 2 of Mhc	Rat	1:200	Babraham MAC 147	Fyrberg et al., 1990
Obscurin	Obscurin (Ig14-16)	Epitope is located in the Ig14-Ig15-Ig16 region	Rabbit	1:400	Belinda Bullard	Burkart et al., 2007
Obscurin	Obscurin (Kin1)	Rabbit antibody was raised against kinase1 domain.	Rabbit	1:400	Belinda Bullard	Katzemich et al., 2012
Profilin	Profilin	Antibody was raised against the full-length chickadee sequence; "chi 1J"	Mouse	1:10	DSHB	Verheyen and Cooley, 1994
Projectin	Projectin (Ig26)	Epitope is located in the Ig26 domain	Rat	1:200	Babraham MAC 150	Lakey et al., 1990
Projectin	Projectin (P5)	Not known	Mouse	1:300	DSHB	Saide et al., 1989
SALS	SALS	Antibody was raised to the 388–594 region; "anti-SALS-Bai"	Rabbit	1:400	Norbert Perrimon	Bai et al., 2007
Sls700	Sls700 (B2)	Epitope is located within a three Ig domain containing region from exon 22	Rabbit	1:200	Belinda Bullard	Burkart et al., 2007
Tmod	Tmod	Not known	Rat	1:200	Velia Fowler	
Tm	Tm	Antibody reacts with Tm (TmH-33 and TmH-34)	Rat	1:400	Babraham MAC 141	Bullard et al., 1988
TmH-34	TmH-34	Antibody reacts with the 34 isoform of TmH Antibody also reacts with GST-2 kin and BiP (hsc72)	Rat	1:200	Babraham MAC 143	Bullard et al., 1988
Tn C	Tn C	Antibody reacts with TnC isoforms F1 and F2 in flight muscle and with Tn C in nonflight muscles	Rat	1:200	Babraham MAC 352	Qiu et al., 2003
Tn T	Tn T	Antibody reacts with TnT in *Lethocerus, Drosophila,* and dragonfly muscles (flight and nonflight)	Rat	1:200	Babraham MAC 145	Bullard et al., 1988
Zasp52	Zasp52	Epitope is located in the sequence encoded by exon 16; "1D3-3E4"	Mouse	1:400	DSHB	Saide et al., 1989
Zormin	Zormin (B1)	Epitope is located in the Ig4-Ig5-Ig6 region; "B1"	Rabbit	1:200	Belinda Bullard	Burkart et al., 2007
α-Actinin	α-Actinin	Monoclonal antibody reacts with α-Actinin	Rat	1:200	Babraham MAC 276	Lakey et al., 1990

Provided online is a supplemental figure PDF showing an overview of the imaged sarcomeric proteins. A representative CLSM image, a collection of representative individual dSTORM images, and an aligned and averaged dSTORM image is presented for every antibody. Scale bar, 500 nm. Measured epitope distributions relative to the Z- or M-line, depicted as violin plots (mean ± SD), are shown on the right. Mean values are indicated with red dots. Schematic diagrams of the depicted proteins are drawn to scale (on the left). The important domains are represented on enlarged diagrams where appropriate. Known epitope positions are also indicated in purple and cyan lines (see also Table S1). The corresponding protein structures are generally presented as in the models (using the same color code), with the exception of the large modular proteins, which are straightened to demonstrate their length. Arrows on the rightmost (upper and lower) individual dSTORM images of Zasp52 indicate regions where a double-line-type distribution can be appreciated. More detailed explanations are provided for each molecule and measurement in the main text and the model constructing part of Materials and methods. Scale bar, 10 nm.

References

Amândio, A.R., P. Gaspar, J.L. Whited, and F. Janody. 2014. Subunits of the Drosophila actin-capping protein heterodimer regulate each other at multiple levels. *PLoS One.* 9:e96326. https://doi.org/10.1371/journal.pone.0096326

Bai, J., J.H. Hartwig, and N. Perrimon. 2007. SALS, a WH2-domain-containing protein, promotes sarcomeric actin filament elongation from pointed ends during Drosophila muscle growth. *Dev. Cell.* 13:828–842. https://doi.org/10.1016/j.devcel.2007.10.003

Bullard, B., K. Leonard, A. Larkins, G. Butcher, C. Karlik, and E. Fyrberg. 1988. Troponin of asynchronous flight muscle. *J. Mol. Biol.* 204:621–637. https://doi.org/10.1016/0022-2836(88)90360-9

Burkart, C., F. Qiu, S. Brendel, V. Benes, P. Håååg, S. Labeit, K. Leonard, and B. Bullard. 2007. Modular proteins from the Drosophila sallimus (sls) gene and their expression in muscles with different extensibility. *J. Mol. Biol.* 367:953–969. https://doi.org/10.1016/j.jmb.2007.01.059

Fyrberg, E., C.C. Fyrberg, C. Beall, and D.L. Saville. 1990. Drosophila melanogaster troponin-T mutations engender three distinct syndromes of myofibrillar abnormalities. *J. Mol. Biol.* 216:657–675. https://doi.org/10.1016/0022-2836(90)90390-8

Katzemich, A., N. Kreisköther, A. Alexandrovich, C. Elliott, F. Schöck, K. Leonard, J. Sparrow, and B. Bullard. 2012. The function of the M-line protein obscurin in controlling the symmetry of the sarcomere in the flight muscle of Drosophila. *J. Cell Sci.* 125:3367–3379. https://doi.org/10.1242/jcs.097345

Kulke, M., C. Neagoe, B. Kolmerer, A. Minajeva, H. Hinssen, B. Bullard, and W.A. Linke. 2001. Kettin, a major source of myofibrillar stiffness in Drosophila indirect flight muscle. *J. Cell Biol.* 154:1045–1057. https://doi.org/10.1083/jcb.200104016

Külshammer, E., and M. Uhlirova. 2013. The actin cross-linker Filamin/Cheerio mediates tumor malignancy downstream of JNK signaling. *J. Cell Sci.* 126:927–938. https://doi.org/10.1242/jcs.114462

Lakey, A., C. Ferguson, S. Labeit, M. Reedy, A. Larkins, G. Butcher, K. Leonard, and B. Bullard. 1990. Identification and localization of high molecular weight proteins in insect flight and leg muscle. *EMBO J.* 9:3459–3467. https://doi.org/10.1002/j.1460-2075.1990.tb07554.x

Li, M.G., M. Serr, K. Edwards, S. Ludmann, D. Yamamoto, L.G. Tilney, C.M. Field, and T.S. Hays. 1999. Filamin is required for ring canal assembly and actin organization during Drosophila oogenesis. *J. Cell Biol.* 146:1061–1074. https://doi.org/10.1083/jcb.146.5.1061

Matusek, T., A. Djiane, F. Jankovics, D. Brunner, M. Mlodzik, and J. Mihály. 2006. The Drosophila formin DAAM regulates the tracheal cuticle pattern through organizing the actin cytoskeleton. *Development.* 133:957–966. https://doi.org/10.1242/dev.02266

Qiu, F., A. Lakey, B. Agianian, A. Hutchings, G.W. Butcher, S. Labeit, K. Leonard, and B. Bullard. 2003. Troponin C in different insect muscle types: identification of two isoforms in Lethocerus, Drosophila and Anopheles that are specific to asynchronous flight muscle in the adult insect. *Biochem. J.* 371:811–821. https://doi.org/10.1042/bj20021814

Saide, J.D., S. Chin-Bow, J. Hogan-Sheldon, L. Busquets-Turner, J.O. Vigoreaux, K. Valgeirsdottir, and M.L. Pardue. 1989. Characterization of components of Z-bands in the fibrillar flight muscle of Drosophila melanogaster. *J. Cell Biol.* 109:2157–2167. https://doi.org/10.1083/jcb.109.5.2157

Shwartz, A., N. Dhanyasi, E.D. Schejter, and B.Z. Shilo. 2016. The Drosophila formin Fhos is a primary mediator of sarcomeric thin-filament array assembly. *eLife.* 5:e16540. https://doi.org/10.7554/eLife.16540

Verheyen, E.M., and L. Cooley. 1994. Profilin mutations disrupt multiple actin-dependent processes during Drosophila development. *Development.* 120:717–728.